Fourier-Based Inspection of Free-Form Reflective Surfaces

Y. Caulier[1] and S. Bourennane[2]

[1] Fraunhofer Institut für Integrierte Schaltungen IIS
Am Wolfsmantel 33, D-91058 Erlangen, Germany
[2] GSM, Institut Fresnel, CNRS-UMR 6133,
École Centrale Marseille, Université Aix-Marseille III, Marseille Cedex 20, France
yannick.caulier@iis.fraunhofer.de, salah.bourennane@fresnel.fr

Abstract. A general free-form surface inspection approach relying on the projection of a structured light pattern and the interpretation of the generated stripe structures by means of Fourier-based features is proposed in this paper.

The major concerns of this paper are the determination of various refrence sets of stripe patterns, and the detailed investigation on the subset of Fourier features that best characterizes free-form bright/dark structures. In order to tackle the inspection problem with a general approach, a first part of this paper is dedicated to the definition of different image data sets that correspond to various types of free-form specular shapes recorded with a structured illumination. A second part deals with the optimization of the most appropriate pattern recognition process. The optimization is dedicated to the use of different pattern arrangements, and the evaluation of different Fourier feature subsets.

It is shown that with only 10 Fourier features and a certain pattern arrangement, high classification rates of free-form surfaces can be obtained.

1 Introduction

Primary purpose of machine vision systems is to provide industrially rugged and cost-effective inspection solutions, they ensure real-time detection, identification and rejection of production defects and serve as valuable process feedback and control utilities. The objects to be inspected usually have complex structures, so that a broad range of different industrial workpieces, as large steel plates [1], steel blocks [2], or bearing rolls [3], can be tackled within the context of industrial quality control processes. Moreover, surface defects can have different shapes, sizes, and physical aspects. Thus, the difficulty within the machine vision domain is to build "intelligent" vision systems which must be at least as good as the human inspector in terms of quality control.

The visual enhancement of a certain type of defective surfaces is, in general, directly dependant of the lighting and the recording technology. Typically, depth defects related to a geometric deformations of the surface, or textural defects

J. Blanc-Talon et al. (Eds.): ACIVS 2008, LNCS 5259, pp. 125–136, 2008.

synonymous of different surface roughness have to be visually enhanced by means of a structural and a diffuse lighting. Different automatic inspection systems have been proposed recently. The firm Aceris [4] proposes a combined 3D laser technique with a 2D colour approach for the measurement of electronic devices. In the same manner, a combined 3D computer tomography technique and a 2D X-Ray sensor are merged in one system of the firm Comet [5].

With the same objective of increasing different defect types with one system, an alternative surface inspection procedure for the characterization of cylindrical objects, is proposed in [6]. It has been demonstrated that the projection of a structured light pattern on the surface to be inspected by means of an adapted illumination serves its direct characterization in terms of defective surfaces visual enhancement. However, in order to simplify the processing of the stripe images, periodical and vertical bright/dark structures have been considered.

Such results are therefore only applicable in case of the characterization of vertical stripe patterns.

There are two possible steps toward the generalization of the proposed inspection method to free-form surfaces. First possible alternative could be to adapt the structured illumination to the shape of the surface to be inspected so that a periodical vertical pattern is depicted in the recording sensor. This approach is difficult or even impossible to implement, in particular if the free-form surfaces are highly specular. This problematic is addressed in detail in [7]. Second possible solution could be to consider the characterization of non-vertical and non-periodical bright/dark structures which are produced when a light pattern is projected onto free-form surfaces. This approach is tackled in this paper.

Most of the research on the definition of adapted stripe-specific features for identification and classification purpose of defective work-pieces are related to the bright/dark patterns obtained with a coherent lighting. Most of the proposed stripe characterization techniques are Fourier- [8,9] or wavelet-based [10,11]. Indeed such transformations, as the Fourier *e.g.*, have the property of periodic features description, which makes such an approach very attractive in terms of the characterization of periodic or almost periodic structures. Within the surface inspection field, [12] uses the inverse Fourier transform to remove the repetitive periodic patterns of statistical features. Qian *et al.* [13] proposes a fault detection method by means of interferometric fringe patterns based on the a windowed Fourier transform approach.

Furthermore, the Fourier method is an attractive approach as far as the computation costs are concerned. The Fast Fourier Transform (FFT) is often used in real-time application processes. [14] proposes a Fourier-based approach for the description of industrial surface defects, and demonstrates that such a technique is accurate and computationally light. Ünsalan [15] uses Fourier-based features for the description of steel surfaces and the FFT to increase the speed of the transformation. [16] *et al.* propose two efficient algorithms to analyze large scale periodic structures by means of FFT-based methods.

With the interpretation of vertical bright/dark structures obtained by means of a non-coherent lighting, the investigations in [17] showed that, as far as the

classification rates of a certain type of defects is concerned, one of the most efficient method was the Fourier-based image content description method.

All these facts concerning the Fourier transform, are strong arguments in favor of using such an approach for stripe image content description. Thus, in case of the inspection task of free-form surfaces, textural Fourier-based features will be used.

The rest of this paper is organized as follows. The 9 different sets of reference stripe image patterns are introduced in Sect. 2. The Fourier-based image content description method is presented in Sect. 3. Sect. 4 briefly introduces the involved classification rule and the classification methodology. The classification results are described in detail in Sect. 5. Finally, a summary is given in Sect. 6.

2 Proposed Method for Free-Form Surface Characterization

The surface inspection principle based on the projection of a structured light pattern, and its characterization in the corresponding images have been introduced in Sect. 1. Such an inspection procedure, was initially defined for the characterization of cylindrical and specular surfaces [6]. The aim is now to apply this inspection principle to a broader range of surface geometries.

As a matter of fact, if non-planar object surfaces are recorded with a conventional planar structured lighting or if the illumination is not adapted to the geometry of the shape being inspected, the bright and dark stripes in the images will neither be vertical nor periodical. Rather, their geometries will depend on the shape of the inspected objects. As a consequence, with the purpose of generalizing the inspection principle to free-form specular surfaces, an extensive range of stripe structures have to be considered. Such stripe geometries can be obtained by means of different surface shapes, structured light positions or sensor types. Our task is not to enumerate all possible combinations of these components and to compute the corresponding stripe geometries. This would be hardly possible. Hence, in order to generalize the proposed inspection method, it is preferable to focus our investigations on a restricted and predefined number of stripe deformations.

A further generalization of the proposed inspection method is dedicated to the arrangement of the patterns to classify, i.e. their arrangement according to the predefined classes. The involved stripe image characterization technique described in [17], allows to discriminate between non-defective and defective 3D depth defects without knowledge of the defect depth. Hence, such a method $2\frac{1}{2}$D surface inspection approach allows the direct discrimination of two distinct 3D defect classes. However, purpose of conventional structured-illumination-based techniques is the depth recovery of the inspected scene [18,19]. Thus, it could be possible to combine the proposed $2\frac{1}{2}$D inspection method with a 3D scene reconstruction technique, and therefore to consider only one 3D class encompassing the defective and the non-defective surfaces. As a consequence, a combined image content description method and depth retrieval approach allows to

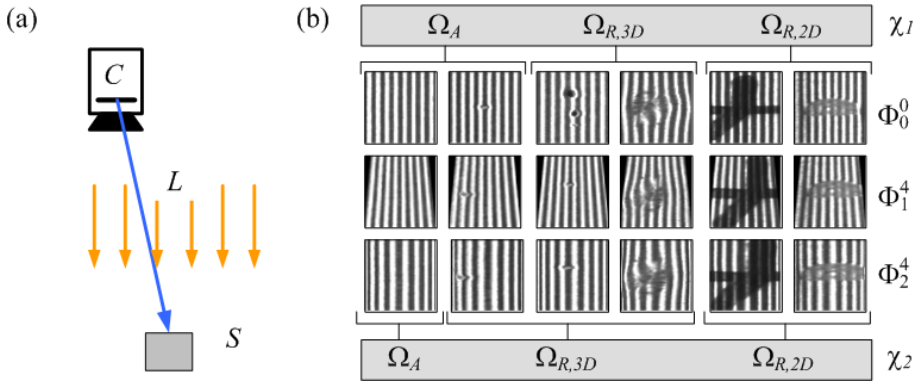

Fig. 1. (a) Surface inspection principle: a camera C records the object surfaces to be inspected S, illuminated by an illumination L, (b) Reference patterns for the classification of free-form surfaces. Image patterns of three different surface shapes -0-, -1- and -2-. Φ_0^0 corresponds to patterns without distortion. Φ_1^4 corresponds to patterns with a maximal perspective distortion of type -1-. Φ_2^4 corresponds to patterns with a maximal cylindrical distortion of type -2-. Φ_1^4 and Φ_2^4 were artificially obtained by warping the images of set Φ_0^0 to simulate the required distortions. All the patterns of al sets have a size of 64×64 pixels. Two different approaches, χ_1 and χ_2, for the classification of classes $\{\Omega_A, \Omega_{R,3D}, \Omega_{R,2D}\}$ were addressed. χ_1 corresponds to the inspection task defined in [6], χ_2 considers all the defective 3D surfaces as belonging to class $\Omega_{R,3D}$.

reconsider the three classes problem and to classify the image patterns according to the depicted disturbances.

Fig. 1 depicts the surface inspection principle and a fraction of reference patterns that are considered in this paper. Two types -1- and -2- of stripe deformations and two pattern arrangements χ_1 and χ_2 are considered. All the patterns are manually annotated and classified into three distinct classes Ω_A, $\Omega_{R,3D}$, and $\Omega_{R,2D}$. These classes correspond to non-defective surfaces, defective 3D geometrical, and defective 2D textural surfaces.

Φ_0^0 is the reference stripe patterns that have been involved for the qualification of the industrial system [6]. This set is made of 252 elements manually annotated and classified into three distinct classes Ω_A, $\Omega_{R,3D}$, and $\Omega_{R,2D}$. Fig. 1 depicts six examples of the reference set Φ_0^0 .

Concerning the inspection of free-form surfaces, two types of pattern structures -1- and -2- are considered. The easiest and simplest way consists of using the patterns of Φ_0^0 and to "transform" or "adapt" them, so that these can be used for the characterization of free-form surfaces. Further derived 8 patterns sets are build from Φ_1^4 . The 4 sets Φ_1^1-Φ_1^4 correspond to the warping of all patterns of Φ_0^0 with increasing projective transformations. The 4 sets Φ_2^1-Φ_2^4 correspond to the warping of all patterns of Φ_0^0 with increasing cylindrical transformations.

Concerning the inspection of two types of pattern arrangements. The 9 image sets are classified according to arrangement χ_1, corresponding to the $2\frac{1}{2}$D direct

surface interpretation approach, and arrangement χ_2, which states for the combined $2\frac{1}{2}$D and 3D depth recovery methodology. In that case, all the 3D defects as defective (all lead to similar disturbances) in a first time. Then, a further step would consists of discriminating the non-defective from the defective parts according to their computed depth.

3 Fourier-Based Stripe Image Content Description

Once the different reference sets have been introduced, the next step consists of defining the most appropriate algorithmic procedures that best characterize the content of such patterns. This is equivalent to search for adequate feature sets that best describe the bright/dark structures depicted in the stripe patterns.

3.1 Definition of the Fourier Transform

The Fourier transform $\mathcal{F}$is a transformation between an input space (spatial domain) into an output space (frequency domain). It's inverse is called the inverse Fourier transform $\mathcal{F}^{-1}$. The Fourier transform is a generalization of the theory of Fourier series and is applicable to all non-periodical and integrable functions.

For a discrete image $\mathbf{F}$ the Fourier transform $\hat{\mathbf{F}} = \mathcal{F}(\mathbf{F})$ and the inverse transform $\mathbf{F} = \mathcal{F}^{-1}(\hat{\mathbf{F}})$ are described by following equations:

$$\hat{\mathbf{F}} = = \sum_{k=0}^{M_u-1} \sum_{l=0}^{M_v-1} f(k,l) e^{-j\frac{2\Pi\kappa}{M_u}k} e^{-\frac{j2\Pi\lambda}{M_v}l}$$
$$\kappa = 0, 1, ..., M_u - 1; \quad \lambda = 0, 1, ..., M_v - 1 \tag{1}$$
$$\mathbf{F} = = \frac{1}{M_u M_v} \sum_{\kappa=0}^{M_u-1} \sum_{\lambda=0}^{M_v-1} \hat{f}(\kappa,\lambda) e^{j\frac{2\Pi k}{M_u}\kappa} e^{j\frac{2\Pi l}{M_v}\lambda}$$
$$k = 0, 1, ..., M_u - 1; \quad l = 0, 1, ..., M_v - 1 \tag{2}$$

f is a two-dimensional function whose values are related to the image $\mathbf{F}$ grey levels. $f(k,l)$ and $f(\kappa,\lambda)$ correspond to the grey level values of images $\mathbf{F}$ and $\hat{\mathbf{F}}$ at positions (k,l) and (κ,λ). M_u and M_v are the width and height of $\mathbf{F}$ and $\hat{\mathbf{F}}$ in pixel. An important remark considering the Fourier transform is that if the samples of the input time image $\mathbf{F}$ are real values $f(k,l) \in \mathbb{R}$, the samples of the output frequency image $\hat{\mathbf{F}}$ are complex values $\hat{f}(\kappa,\lambda) \in \mathbb{C}$ so that the information of a Fourier transformed image is contained in the magnitude and the phase of the spectral representation. In many applications only the magnitude information is needed and the phase information is discarded. However, despite this common practice, in some context phase information should not be ignored. Oppenheim and Lim [20] have shown that if we construct synthetic images made from the magnitude information of one image and the phase information of another, it is the image corresponding to the phase data that we perceive, if somewhat degraded.

In our case we will only consider the magnitude of the Fourier transform, noted $|\hat{\mathbf{F}}|$. Its representation is done in a cartesian coordinate system whose $\nu_\mathbf{1}$-axis is horizontal with ascendant values from left to right and $\nu_\mathbf{2}$-axis is vertical with ascendant values from top to bottom. Images $\mathbf{F}$ and $|\hat{\mathbf{F}}|$ have the same dimensions.

3.2 Texture Analysis with Fourier Transform

We apply the method proposed by Weska [21] which uses different parts of the frequency spectrum for classification purposes. The characterization of the image pattern $\mathbf{F}$ is based on the Fourier power spectrum $\mathbf{P}$ which is defined as the square of the spectral's magnitude $|\hat{\mathbf{F}}|$. $\mathbf{P}$ is a matrix of same size as matrix $\hat{\mathbf{F}}$, $\mathbf{P}(\kappa, \lambda)$ is the value of the power spectrum at position (κ, λ). We have following definition:

$$\begin{aligned} \mathbf{P} &= |\hat{\mathbf{F}}|^2 \\ \mathbf{P}(\kappa,\lambda) &= |\hat{f}(\kappa,\lambda)|^2, \quad \kappa \in 0,1,\cdots,M_u-1; \quad \lambda \in 0,1,...,M_v-1 \end{aligned}$$

The power spectrum is used as an image signature for the discrimination of different types of stripe images. Weska considers the radial and the angular spectral distributions, saying that the former is sensitive to texture coarseness and the latter to texture directionality. Weska also uses the distributions corresponding to the principal spectral image axes, the ν_1- and ν_1-directions. The mathematical expression of the four spectral regions is shown in Fig. 2.

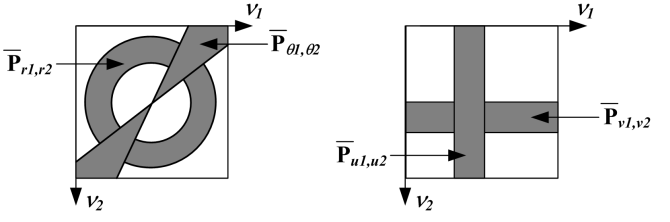

$$\overline{\mathbf{P}}_{r_1,r_2} = \sum_{\begin{bmatrix} r_1^2 \le \kappa^2+\lambda^2 < r_2^2 \\ 0<\kappa<\frac{M_u}{2}; 0<\lambda<\frac{M_v}{2} \end{bmatrix}} |\hat{f}(\kappa,\lambda)|^2 \quad \overline{\mathbf{P}}_{v_1,v_2} = \sum_{\begin{bmatrix} 0<\kappa<M_u \\ v_1<\lambda<v_2 \end{bmatrix}} |\hat{f}(\kappa,\lambda)|^2$$

$$\overline{\mathbf{P}}_{\theta 1\,\theta 2} = \sum_{\begin{bmatrix} \theta_1 \le tan^{-1}(\lambda/\kappa) < \theta_1 \\ 0<\kappa<\frac{M_u}{2}; 0<\lambda<\frac{M_v}{2} \end{bmatrix}} |\hat{f}(\kappa,\lambda)|^2 \quad \overline{\mathbf{P}}_{u_1,u_2} = \sum_{\begin{bmatrix} u_1<\lambda<u_2 \\ 0<\kappa<M_v \end{bmatrix}} |\hat{f}(\kappa,\lambda)|^2$$

Fig. 2. Partitioning principle of the frequency domain for the computing of the 33 regions of the power spectrum

The assumption using different parts of the power spectrum is that some regions may be more discriminative or representative of certain classes of stripe images. Such images are characterized by a vertical pattern whose disturbances are synonymous of defective surfaces. Hence, we guess that isolating the regions of the power spectrum which correspond to the vertical stripe pattern for the computation of the characteristic features could lead to better classification rates.

3.3 Fourier-Based Classification

For the purposes of this paper a total number of 33 features corresponding to the average value of power spectrum regions are used. A total of 8 radial regions with $\overline{\mathbf{P}}_{r1,r2}$, 10 directional regions with $\overline{\mathbf{P}}_{\theta 1,\theta 2}$, 5 horizontal regions with $\overline{\mathbf{P}}_{v1,v2}$ and 10 vertical regions with $\overline{\mathbf{P}}_{u1,u2}$ is considered. The number of computed features is independent of the size of the image pattern. Mathematical formulation of the 5 involved feature vectors $\mathbf{c}^F_{r,\theta,v,u}$, $\mathbf{c}^F_r$, $\mathbf{c}^F_\theta$, $\mathbf{c}^F_v$, and $\mathbf{c}^F_u$ are as follows:

$$
\begin{aligned}
&\mathbf{c}^F_{r,\theta,v,u} = \{\{\overline{\mathbf{P}}_{r1,r2}\},\{\overline{\mathbf{P}}_{\theta 1,\theta 2}\},\{\overline{\mathbf{P}}_{v1,v2}\},\{\overline{\mathbf{P}}_{u1,u2}\}\}, \quad \mathbf{c}^F_{r,\theta,v,u} \in \mathbb{R}^{33}\\
&\mathbf{c}^F_{r,\theta,v,u} = \{\{\mathbf{c}^F_r\},\{\mathbf{c}^F_\theta\},\{\mathbf{c}_v\},\{\mathbf{c}^F_u\}\}\\
&\text{with} \quad \{\overline{\mathbf{P}}_{r1,r2}\} \in \mathbb{R}^8, \{\overline{\mathbf{P}}_{\theta 1,\theta 2}\} \in \mathbb{R}^{10}, \{\overline{\mathbf{P}}_{v1,v2}\} \in \mathbb{R}^5, \{\overline{\mathbf{P}}_{u1,u2}\} \in \mathbb{R}^{10}\\
&\text{and} \quad (r_1;r_2) = (jr;(j+1)r), \;\; r = (\tfrac{M_u}{2}{}^2 + \tfrac{M_v}{2}{}^2)/8, j = \{0,...,7\} \qquad (3)\\
&\qquad\quad (\theta_1;\theta_2) = (j\theta;(j+1)\theta), \;\; \theta = 2\pi/10, \qquad j = \{0,...,9\}\\
&\qquad\quad (v_1;v_2) = (jv;(j+1)v), \;\; v = \tfrac{M_v}{2}/5, \qquad j = \{0,...,4\}\\
&\qquad\quad (u_1;u_2) = (ju;(j+1)u), \; u = \tfrac{M_u}{2}/10, \qquad j = \{0,...,9\}
\end{aligned}
$$

The classification of the stripe patterns is evaluated by using all 33 features of vector $\mathbf{c}^F_{r,\theta,v,u}$ but also by considering the radial, angular, horizontal or vertical regions of the power spectrum separately, *i.e.* by means of the four different feature vectors $\mathbf{c}^F_r \in \mathbb{R}^8$, $\mathbf{c}^F_\theta \in \mathbb{R}^{10}$, $\mathbf{c}^F_v \in \mathbb{R}^5$, and $\mathbf{c}^F_u \in \mathbb{R}^{10}$.

4 Pattern Classification

Pattern classification process consists of applying a *classification rule* and a certain *classification methodology* to automatically assign a class Ω to a pattern $\mathbf{F}$, so that the classification rates are maximized, *i.e.* the false alarms rates are minimized. A tremendous number of possible pattern classification rules, as the statistic-based [22,23,24], or the instance-based [25,26,27] are described in the pattern analysis literature. In the same manner, various classification methodologies, as the n-fold cross-validation, or the Bootstrap approaches [28,29,30] are proposed within the pattern analysis literature.

Testing the influence of various pattern classification approaches would be beyond the scope of this paper. Thus, it is necessary to select the most adequate classification rule and an appropriate classification methodology in terms of stripe pattern interpretation.

Concerning the feature-based interpretation of stripe structures, three different rules were considered in [17]: the Naive Bayes, the One-Nearest-Neighbor and the Three-Nearest-Neighbor. Their influence on the classification of vertical periodical bright/dark structures was evaluated. The comparison of these three classificators showed that, in general better classification rates were obtained using the One-Nearest-Neighbor approach. This is a strong argument in terms of using "only" this approach for our purposes. Furthermore, Cover [31] and Guttierez [32] show that the k-NN method approaches the results of the Naive Bayes classifier in case of a large data set as we have here.

With the methodology, a 10-fold stratified validation, which is certainly the mostly used approach within the pattern classification community, was addressed in [17]. Various n-fold cross-validation approaches for different values of n has been evaluated and compared with the bootstrap technique by Kohavi [33]. He shows that a stratified 10-fold cross-validation is the more appropriate model in terms of classification accuracy. Moreover, Witten [28], referred that a ten times sampling is the right number of folds to get the best estimation error.

Thus, as our aim is to evaluate the two proposed Fourier sets of features *and not* a certain stripe pattern classification, we "only" consider the 1-NN classification rule combined with a stratified 10-fold cross-validation for our purposes.

5 Classification Results

This section is dedicated to the evaluation and comparison of the different involved feature sets using the 33 Fourier characteristics. The final purpose is to extract a subset of features, as small as possible to retrieve only the most relevant features that accurately classifies the reference image sets. The evaluation criteria for each set of pattern is the rate R of correctly classified patterns, expressed in percent.

With the purpose of optimizing the proposed Fourier-based pattern characterization process, a primary feature selection or feature subset evaluation process is necessary. The purpose is to determine which of the 4 subsets introduced in Sect. 3 are particulary relevant for the characterization of the stripe structures.

5.1 Fourier Subsets Evaluation

Table 1 shows the classification results of image set Φ_0^0 by means of vector $\mathbf{c}^{\mathrm{F}}_{r,\theta,v,u}$ made of the 33 Fourier features, and the 4 feature subset vectors described in equation (3).

In section 3.3 the assumption was made that some frequency subbands could be more representative of the stripe patterns to be characterized. This is clearly observable in case of the results listed in Table 1. A high discrepancy in the classification results is observable concerning the Fourier-based approach. Best classification rates of 90.4% and 92.4% are obtained when only the 10 directional Fourier features $\mathbf{c}^{\mathrm{F}}_{\theta}$ are used.

These results show that from the 33 Fourier features, the subset made of the 10 directional Fourier features is particulary relevant in terms of stripe pattern

Table 1. Rates R of correctly classified patterns for image set Φ_0^0 with Fourier's textural features by means of a 1-NN classifier. The two pattern arrangements χ_1 and χ_2 are considered.

Feature vector	Arrangement χ_1	Arrangement χ_2
$\mathbf{c}^{\mathrm{F}}_{r,\theta,v,u}$	85.7	87.7
$\mathbf{c}^{\mathrm{F}}_{r}$	79.7	79.3
$\mathbf{c}^{\mathrm{F}}_{\theta}$	90.4	92.4
$\mathbf{c}^{\mathrm{F}}_{v}$	84.1	83.3
$\mathbf{c}^{\mathrm{F}}_{u}$	84.1	86.5

characterization. Thus, further investigations are dedicated to the characterization of free-form surface using the 33 Fourier, the 10 directional Fourier.

5.2 Free-Form Surface Characterization

Fig. 3 shows the classification rates for image distortions of type -1- and of type -2- by means of the three feature vectors $\mathbf{c}^{\mathrm{F}}_{r,\theta,v,u}$, $\mathbf{c}^{\mathrm{F}}_{\theta}$, and for pattern arrangements χ_1 and χ_2.

These graphics confirm the results of Table 1, *i.e.* that the selective use of only the Fourier directional features lead to more accurate classification rates. In particular as far as the second type of stripe distortions -2- is concerned.

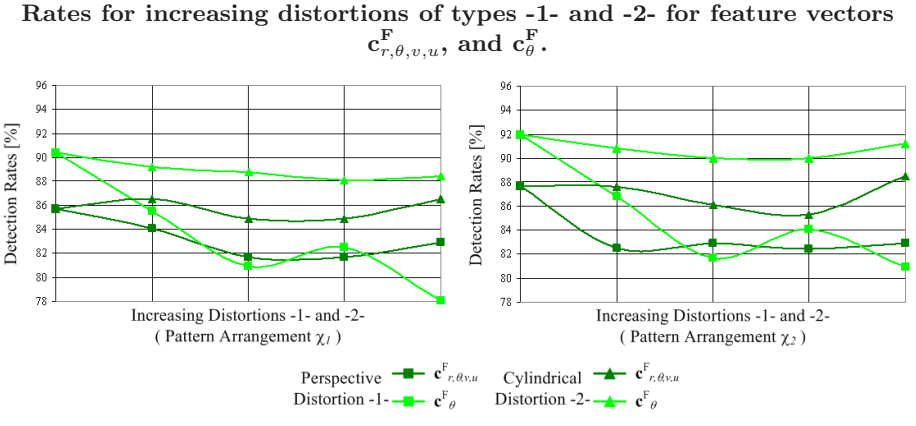

Fig. 3. The detection rates are computed for different image sets and correspond to increasing distortions of type -1- and of type -2-. Left values on the axis of abscissae: detection rates for image set Φ_0^0 . Right values on the axis of abscissae: detection rates for image sets Φ_1^4 and Φ_2^4 .

The results are not similar for both pattern arrangements. Indeed, the classification rates are slightly better in case of a combined $2\frac{1}{2}$D / 3D approach, *i.e.* for arrangement χ_2, where a lowest rate of 81 % for all set of patterns is observed. In case of arrangement χ_1, the lowest rate is 78 %.

6 Summary

Based on a method initially defined for the automatic inspection of cylindrical specular surfaces, a general approach for the characterization of free-form specular shapes is proposed in this paper. The inspection principle relies on the interpretation of a stripe pattern projected onto the surface to be inspected and recorded by the optical sensor.

Starting from the reference image set defined for the qualification of the industrial process, 8 additionally image sets, corresponding to various types of free-form specular shapes recorded with a structured illumination could be defined. All these image sets are used to search for the most appropriate Fourier features.

With respect to the characterization of periodic or almost periodic bright/dark structures, a Fourier-based image-content description method defined within the texture analysis field, is considered. In order to propose a general approach to the inspection method, two different types of stripe deformations, and two different pattern arrangements are considered.

The Fourier method necessitates the computation of a huge amount of 33 features, which signifies high computational costs. Hence, in order to propose a competitive, real-time able inspection procedure, extensive investigations are done to retrieve only the most relevant features that accurately classifies all the reference image sets.

Finally, it is demonstrated that with only the 10 directional Fourier features high classification rates can be reached. Moreover, it is shown that the pattern arrangement has a direct influence on the detection accuracy. In case of the proposed inspection task relying on a structured illumination, a combined 2 $2\frac{1}{2}$D / 3D approach is prefered.

References

1. Grunditz, C.H., Walder, M., Spaanenburg, L.: Constructing a Neural System for Surface Inspection. In: Proc. of IEEE Int. Joint Conf. on Neural Networks, vol. 3, pp. 1881–1886 (2004)
2. Reindl, I., OrsquoLeary, P.: Geometric Surface Inspection of Raw Milled Steel Blocks, pp. 849–856. Springer, Berlin (2004)
3. Pernkopf, F., O'Leary, P.: Visual inspection of machined metallic high-precision surfaces. EURASIP Journal on Applied Signal Processing archive 2002(1), 667–678 (2002)
4. Aceris-3D: FC Substrate Bump Inspection System. Product documentation, Aceris 3D Clark Graham 300, Baie D'Urfe, Québec, Canada (2005)

5. Comet-AG: Feinfocus Fox, High Resolution 2D/3D. Product documentation, Comet AG Herrengasse 10, 31775 Flamatt, Switzerland (2005)
6. Caulier, Y., Spinnler, K., Bourennane, S., Wittenberg, T.: New Structured Illumination Technique for the Inspection of High Reflective Surfaces. EURASIP Journal on Image and Video Processing (2008) doi:10.1155/2008/237459
7. Kammel, K.: Deflektometrische Untersuchung spiegelnd reflektierender Freiformflächen. University of Karlsruhe (TH), Germany (2004)
8. Takeda, M., Ina, H., Kobayashi, S.: Fourier-transform method of fringe-pattern analysis for computer-based topography and interferometry. J. Opt. Soc. Am. 72(1), 156–160 (1982)
9. Qian, K., Seah, H.S., Asundi, A.: Fault detection by interferometric fringe pattern analysis using windowed Fourier transform. Measurement Science and Technology 15, 1582–1587 (2005)
10. Krüger, S., Wernicke, G., Osten, W., Kayser, D., Demoli, N., Gruber, H.: Fault detection and feature analysis in interferometric fringe patterns by the application of wavelet filters in convolution processors. Machine Vision Application in Industrial Inspection 3966(1), 145–153 (2000)
11. Li, X.: Wavelet transform for detection of partial fringe patterns induced by defects in nondestructive testing of holographic interferometry and electronic speckle pattern interferometry. Journal of Optical Engineering 39(1), 2821–2827 (2000)
12. Tsai, D.M., Huang, T.Y.: Automated surface inspection for statistical textures. Image and Vision Computing 21(4), 307–323 (2003)
13. Qian, K., Seah, H.S., Asundi, A.: Fringe 2005: Fault detection from temporal unusualness in fringe patterns. Stutgart, Germany (2005)
14. Kunttu, I., Lepistö, L., Rauhamaa, J., Visa, A.: Fourier-Based Object Description in Defect Image Retrieval. Machine Vision Applications 17(4), 211–218 (2006)
15. Ünsalan, C.: Pattern Recognition Methods for Texture Analysis Case Study: Steel Surface Classification. University of Hacettepe, Turkey (1998)
16. Li, W.B., Cui, T.J., Yin, X., Qian, Z.G., Hong, W.: Fast algorithms for large-scale periodic structures using subentire domain basis functions. IEEE Trans. on antennas and propagation 53(3), 1154–1162 (2005)
17. Caulier, Y., Spinnler, K., Wittenberg, T., Bourennane, S.: Specific Features for the Analysis of Fringe Images. Journal of Optical Engineering 47(5) (2008)
18. Knauer, M.C., Kaminski, J., Haeusler, G.: Phase Measuring Deflectometry: a new approach to measure specular free-from surfaces. Optical Metrology in production Engineering 5457, 366–376 (2004)
19. Kammel, S., Puente, L.F.: Deflektometrie zur Qualitätsprüfung spiegelnd reflektierender Oberflächen. Technisches Messen 70, 193–198 (2003)
20. Oppenheim, A.V., Lim, J.S.: The importance of Phase in Signals. Proc. of the IEEE 69(5), 529–541 (1981)
21. Weska, J.S., Charles, R.D., Rozenfeld, A.: A Comparative Study of Texture Measures for Terrain Classification. IEEE Transaction s on Systems, Man, and Cybernetics 6(4), 269–285 (1976)
22. Tang, W.H., Goulermas, J.Y., Wu, Q.H., Richardson, Z.J., Fitch, J.: A Probabilistic Classifier for Transformer Dissolved Gas Analysis With a Particle Swarm Optimizer. IEEE Trans. on Power Delivery 23(2) (2008)
23. Ruiz, A., López-de-Teruel, P.E.: Nonlinear Kernel-Based Statistical Pattern Analysis. IEEE Trans. on Neural Networks 12(1) (2001)
24. Babich, G.A., Camps, O.I.: Weighted Parzen Windows for Pattern Classification. IEEE Trans. on Pattern Anal. and Machine Intell. 18(5) (1996)

25. Foresti, G.L., Micheloni, C.: Generalized Neural Trees for Pattern Classification. IEEE Trans. on Neural Networks 13(6) (2002)
26. Geva, S., Sitte, J.: Adaptative Nearest Neighbor Pattern Classification. IEEE Trans. on Neural Networks 2(2) (1991)
27. Goldstein, M.: k-Nearest Neighbor Classification. IEEE Trans. on Information Theory 18(5) (1972)
28. Witten, I.H., Eibe, F.: Data Mining. Elsevier, Oxford (2005)
29. Kohavi, R.: A Study of Cross-Validation and Bootstrap for Accuracy Estimation and Model Selection. In: Proc. of IJCAI, vol. 3, pp. 1137–1145 (1995)
30. Efron, B., Tibshirani, R.J.: An Introduction to the Bootstrap. Chapman and Hall, New York (1993)
31. Cover, T.M., Hart, P.E.: Nearest Neighbor Pattern Classification. IEEE Trans. on Information Theory 13(1), 21–27 (1967)
32. Gutierrez-Osuna, R.: Wrappers for feature Subset Selection. IEEE Sensors Journal 2(3), 273–324 (2003)
33. Kohavi, R., John, G.H.: A Review. Artificial Intelligence 2(3), 189–202 (2002)